organics

MDPI

Article

Exploration of the Divergent Outcomes for the Nenitzescu Reaction of Piperazinone Enaminoesters

Rebecca Hermans [1], Max Van Hoof [1], Luc Van Meervelt [2] and Wim Dehaen [1,*]

[1] Sustainable Chemistry for Metals and Molecules, Department of Chemistry, KU Leuven, Celestijnenlaan 200F, B-3001 Leuven, Belgium
[2] Biochemistry, Molecular and Structural Biology, Department of Chemistry, KU Leuven, Celestijnenlaan 200F, B-3001 Leuven, Belgium
* Correspondence: wim.dehaen@kuleuven.be

Abstract: The Nenitzescu reaction is a condensation reaction between an enamine and a quinone, which can give rise to a wide variety of reaction products depending on the nature of the starting material and the reaction conditions. The most commonly observed products are 5-hydroxyindoles and 5-hydroxybenzofurans. Both classes are of interest since they are known to possess a variety of promising bioactivities. Despite the high chemodivergency for this reaction, it remains an interesting synthetic strategy thanks to the mild reaction conditions, easily accessible starting materials and simple reaction procedures. For these reasons, our research group investigated the Nenitzescu reaction of piperazinone enaminoesters, resulting in the unexpected formation of rearranged 2-imidazolidinone benzofurans. In this work, we aimed to develop reaction conditions that favor the formation of 5-hydroxyindoles via an extensive, multivariate optimization study. This led to valuable insights into the parameters that influence regio- and chemoselectivity. Furthermore, two novel products were obtained, a pyrrolo[2,3-*f*]indole and a benzofuranone, both of which are rarely reported in the literature.

Keywords: Nenitzescu reaction; piperazinone enaminoesters; 5-hydroxyindole; pyrrolo[2,3-*f*]indole; 5-hydroxybenzofuran-2-one

Citation: Hermans, R.; Van Hoof, M.; Van Meervelt, L.; Dehaen, W. Exploration of the Divergent Outcomes for the Nenitzescu Reaction of Piperazinone Enaminoesters. *Organics* **2023**, *4*, 146–163. https://doi.org/10.3390/org4020012

Academic Editor: David StC Black

Received: 9 February 2023
Revised: 16 March 2023
Accepted: 29 March 2023
Published: 7 April 2023

1. Introduction

The Nenitzescu reaction is the condensation of an enamine and a quinone and is a well-established synthetic pathway towards 5-hydroxyindole and benzofuran derivatives [1,2]. These classes of compounds exhibit promising activities for a variety of pharmaceutic applications, e.g., as antiviral agents [3–10], anti-inflammatory drugs [11–14], anticancer agents [15–17], and anti-arrhythmic agents [18]. This research fits within the research interests of the laboratory of organic synthesis at the Department of Chemistry at KU Leuven concerning the condensation reactions of quinones [19–23].

The Nenitzescu reaction has been successfully carried out under various conditions, including the use of (Lewis) acids, in the absence of acid, with different solvents and at varying temperatures [1,2,24–26]. The course of the reaction depends heavily on the reaction conditions and the structure of the starting materials [1,2,24–26]. Moreover, 5-hydroxyindoles are generally formed in an oxidation-reduction pathway [27–29] (Scheme 1A). The Michael addition of the enamine **2** to the quinone **1** results in an enamino hydroquinone **I1**, which is oxidized to the corresponding quinone **I2** by an appropriate oxidant (e.g., unreacted benzoquinone **1** or oxygen). The enamino quinone **I2** cyclizes to hemiaminal **I3,** after which acid-catalyzed dehydration followed by reduction affords the 5-hydroxyindole **3**. Possible reductants include hydroquinone and enamino hydroquinone **I1**. In apolar solvents and in the presence of Lewis acids (LA), the reaction occurs via an alternative pathway [30] (Scheme 1B). After the addition of the enamine **2** to the Lewis-acid-activated quinone **1′**, the adduct **I5** isomerizes to the activated enamine **I6,** allowing cyclization without prior

oxidation. After ring closure, proton transfer, and Lewis-acid-catalyzed dehydration, indole **3** is obtained. Similar to 5-hydroxyindole formation, the 5-hydroxybenzofuran pathway is initiated with the formation of Michael adduct **I1** [28,31] (Scheme 1C). This adduct is protonated, allowing cyclization to hemiaminal **I10**. Subsequently, an acid-catalyzed amine elimination generates 5-hydroxybenzofuran **4**.

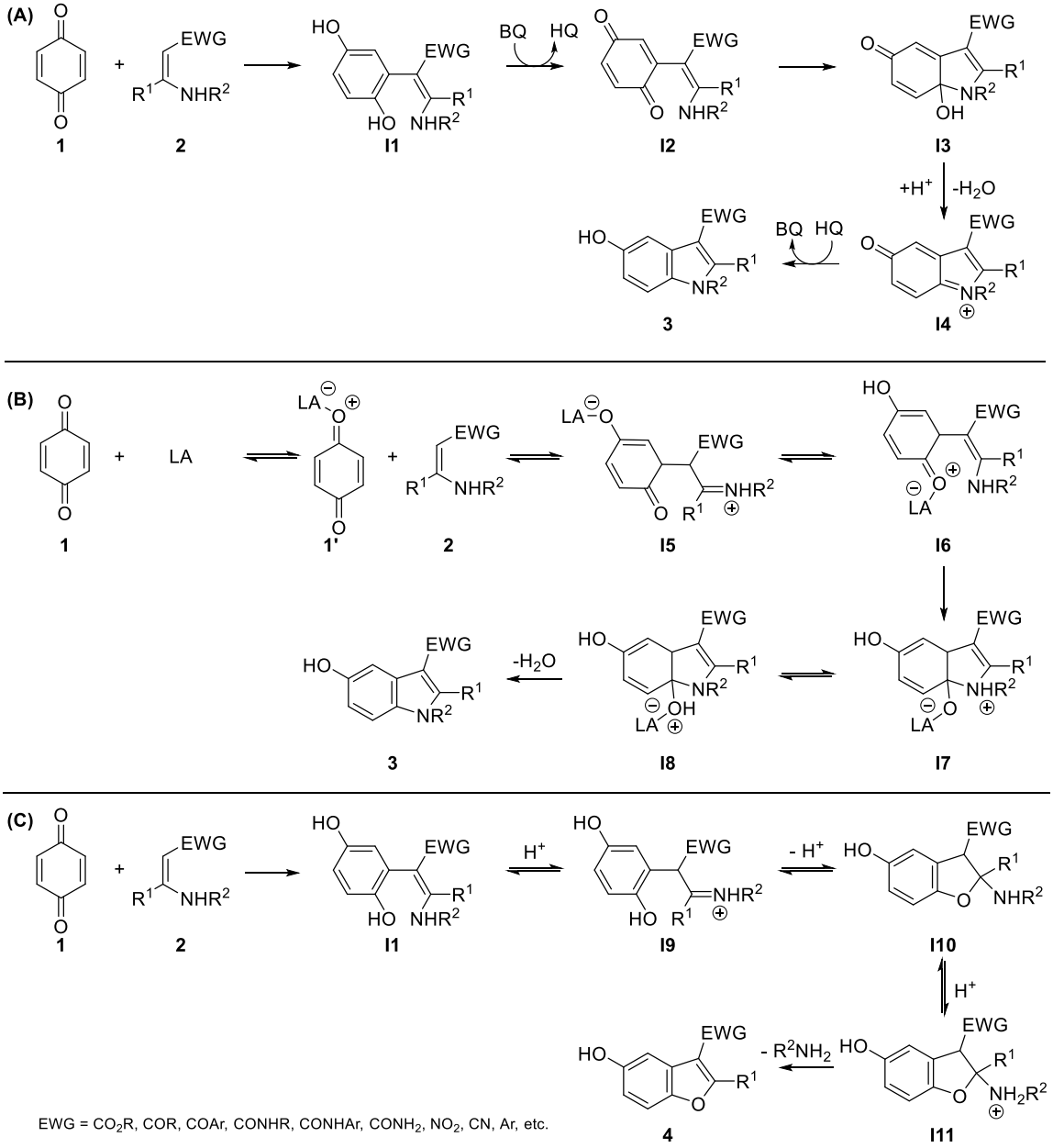

Scheme 1. (**A**) Oxidation-reduction mechanism of the 5-hydroxindole synthesis; (**B**) Mechanism for Lewis-acid-catalyzed 5-hydroxyindole synthesis; (**C**) Mechanism of the 5-hydroxybenzofuran synthesis.

Besides 5-hydroxyindoles and benzofurans, a diverse range of alternative reaction products, including 6-hydroxyindoles [32–34], O-acylated 4,5-dihydroxyindoles [33,35–38], pyrroloindoles [39], furo[2,3-*f*]benzofurans [40], and dimeric indoles [35], have been isolated (Scheme 2). Moreover, 6-hydroxyindoles are formed in the so-called 'anti-Nenitzescu reaction' which occurs via a 1,2-addition followed by an intramolecular Michael addition [15,23]. Especially, reactions of *N*-aryl-substituted enaminoesters at low temperatures are known to generate 6-hydroxyindoles [41]. O-acylated 4,5-dihydroxyindoles are com-

mon (by)products in acetic or propanoic acid [33,35–38], and are formed by the nucleophilic attack of the carboxylate on 5-hydroxyindole intermediate **I4** [33,35–38]. Pyrroloindoles and furo[2,3-*f*]benzofurans derive from the addition of a second enamine to enamino quinone **I2** or hemiaminal **I3** and have been isolated from the reaction of *N*-substituted enamines with *p*-benzoquinone [39,40,42]. Dimeric bisindoles have been obtained from the reaction of *N*-alkyl enaminoesters and *p*-benzoquinone [35].

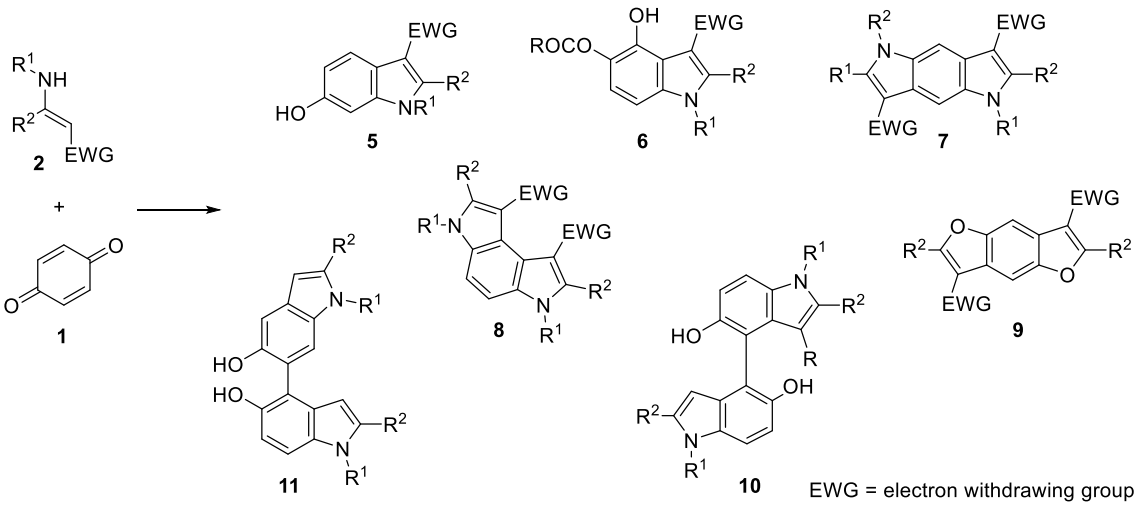

Scheme 2. Overview of alternative reaction products.

Recently, our research group investigated the Nenitzescu reaction of piperazinone enaminoesters [27,43]. This research was inspired by earlier work conducted by Parr and Reiss, who obtained enamino quinone **13** from the condensation of enamine **12** and *p*-benzoquinone, and O-acylated 4,5-dihydroxyindole **14** upon heating in acetic acid [44] (Scheme 3A). Our research group hypothesized that by replacing acetic acid (AcOH) with trifluoroacetic acid (TFA), thus lowering the nucleophilicity of the acetate, the formation of the O-acylated indole could be suppressed allowing the synthesis of a 5-hydroxyindole [23]. Interestingly, the reaction produced an unexpected rearranged 2-imidazolidinonebenzofuran **16** and not the anticipated 5-hydroxyindole (Scheme 3B). The reaction conditions were optimized towards this novel product, and a stochiometric quantity of $BF_3{\cdot}OEt_2$ (1.2 equiv.) in acetonitrile (ACN) was found to be optimal in combination with 2.2 equivalents of benzoquinone. Interestingly, the optimized reaction conditions were also regioselective for the evaluated monosubstituted quinones [27].

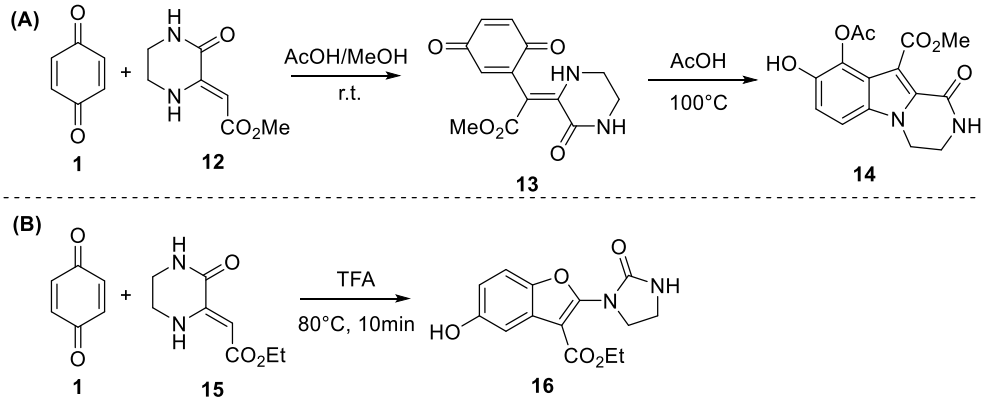

Scheme 3. (**A**) Parr and Reiss, the condensation of a cyclic enamine and *p*-benzoquinone, data from [44]; (**B**) Unexpected formation of a rearranged benzofuran, data from [23].

Besides rearranged benzofurans, enamino quinones and 5-hydroxyindoles were observed under certain conditions, for example, in Et_2O as solvent or when using 2,5-dimethyl-*p*-benzoquinone or tert-butyl-*p*-benzoquinone under the optimized conditions [23].

Considering the interesting properties of 5-hydroxyindoles [3,4,6–11,16,45], in this work the Nenitzescu reaction of enaminoesters was further investigated with the aim of developing regioselective conditions favoring 5-hydroxyindole formation. To this end, an extensive, multivariate screening of reaction conditions was performed using the condensation of piperazinone enaminoester **15** and methyl-*p*-benzoquinone as a model reaction. The use of the latter enabled simultaneous yield and regioselectivity determination by quantitative ^{1}H NMR (^{1}H qNMR). This screening led to new and important insights into the factors that influence regio- and chemoselectivity. Additionally, two unexpected novel products were synthesized: a pyrrolo[2,3-*f*]indole and a benzofuranone.

2. Results and Discussion

Starting from the optimized reaction conditions for benzofuran **16** formation, a multivariate screening was performed, altering solvent, acid mediator, temperature, reaction time and reactant equivalency (Table 1, Scheme 4). This resulted in a deepened understanding of the factors that impact the outcome of the reaction. For instance, it was found that acidic additives greatly affect the regio- and chemoselectivity. Reactions mediated by Lewis and Brönsted acids—$CuCl_2$, $BiCl_3$, $FeCl_3$, $In(OTf)_3$, trifluoroacetic acid (TFA) and triflic acid (TfOH)—afforded only trace amounts of indoles **18a/b** and generated benzofuran **19** as a main cyclization product (Table 1). Zinc halides (ZnI_2, $ZnCl_2$ or $ZnBr_2$) promoted cyclization towards 5-hydroxyindoles in all tested solvents, while scandium and zinc triflate facilitated the formation of a novel product: benzofuranone **21a** (vide infra). Surprisingly, the nature of the halide counterion influenced the regioselectivity significantly. Moreover, 7-methyl-5-hydroxyindole **18a** yields were generally higher with zinc iodide, and 6-methyl-5-hydroxyindole **18b** yields were generally higher with zinc chloride. Additionally, the regioisomeric ratio and overall yield also varied depending on the solvent, and nitromethane was the most suitable for 5-hydroxyindole formation in combination with either zinc chloride or zinc iodide. However, the combined yields were only 26% and 27%, respectively, and large quantities of enamino quinone intermediates **20a/b** were present in the reaction mixture. Varying the reaction temperature, time, catalyst concentration or reagent equivalence did not improve the outcome of the reaction. On the contrary, increasing temperature and catalyst concentration were detrimental for the product yields, regio- and chemoselectivity.

Next to varying reaction conditions, a control experiment with hydroquinone instead of methyl-*p*-benzoquinone was performed using one equivalent hydroquinone and 0.1 equivalent zinc triflate in DCM at 40 °C. As expected, no conversion was observed after 22 h.

As mentioned above, scandium and zinc triflate mediation allowed the formation of an alternative reaction product: benzofuranone **21a** (Scheme 5). Presumably, this heterocycle is formed via the acid-catalyzed lactonization of hydroquinone intermediate **I12** (Scheme 5). This hypothesis is substantiated by the studies of Panisheva et al. and Mikerova et al., which showed that sterically demanding enamino hydroquinones readily cyclize to benzofuranone derivatives in acidic medium [46,47]. Aside from this two-step synthesis via isolated enamino hydroquinones [46,47], benzofuranones have rarely been described as products from the Nenitzescu reaction. Sung et al. reported the formation of benzofuranones via the Blaise–Nenitzescu reaction, which occurs by the condensation of an in situ-generated zinc complexed enaminoester and a quinone [48]. However, the authors were not able to synthesize benzofuranones starting from the isolated enamine (Blaise product). Mbala et al. afforded hydroxybenzo[*g*]furo[4,3,2-*de*]isoquinoline-2,5(4*H*)-diones from the condensation of *N*-substituted enaminoesters with methoxycarbonyl-1,4-naphthoquinone [49]. However, in this condensation an isoquinolinone ring is formed in addition to the benzofuranone ring. So, it can be stated that there is very little/no precedent for benzofuranone formation as a

direct product from the classical Nenitzescu reaction. For this reason, a limited optimization study was undertaken (Table 2). During the optimization, NMR analysis indicated the presence of a small amount of the 6-methyl substituted isomer **21b** in the reaction mixtures, though isolation was unsuccessful.

Table 1. Multivariate screening of reaction conditions, optimization towards 5-hydroxyindoles **18a/b**.

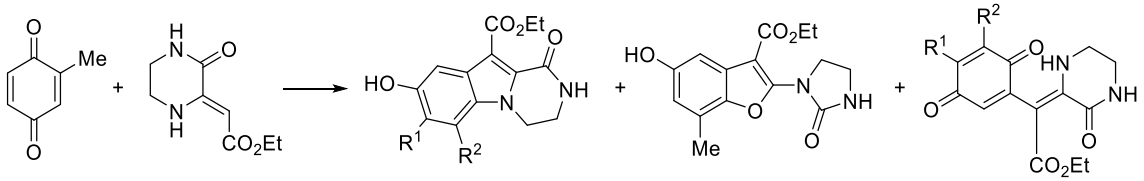

17 **15** **18a:** R^1 = H, R^2 = Me; **18b:** R^1 = Me, R^2 = H **19** **20a:** R^1 = H, R^2 = Me; **20b:** R^1 = Me, R^2 = H

Entry	Solvent	Additive (eq.)	SM 17 (eq.)	Time	T (°C)	Yield [a] (%)		
						18a/b	19	20a/b
1	ACN	$BF_3{\cdot}OEt_2$ (1.2)	2	3 h	r.t.	**18a** (<5)	**19** (55)	**20a** (<5)
2	Et_2O	$BF_3{\cdot}OEt_2$ (1.2)	2	22 h	r.t.	**18a** (7)	**19** (45)	**20b** (10)
3	THF	$BF_3{\cdot}OEt_2$ (1.2)	2	22 h	r.t.	**18a** (<5)	**19** (64)	-
4	DCM	$BF_3{\cdot}OEt_2$ (1.2)	2	22 h	r.t.	**18a** (8); **18b** (<5)	**19** (51)	**20a** (11)
5	DCM	TFA (1.2)	2	22 h	r.t.	**18a** (6)	**19** (20)	**20a** (13); **20b** [b]
6	DCM	TfOH (1.2)	2	22 h	r.t.	**18a** (<5); **18b** (6)	**19** (15)	**20a** (15)
7	DCM	$ZnCl_2$ (1.2)	2	22 h	r.t.	**18a** (<5); **18b** (9)	**19** (<5)	**20a** (41); **20b** (**19**)
8	DCM	$CuCl_2$ (1.2)	2	22 h	r.t.	-	**19** (22)	**20b** (45)
10	DCM	$FeCl_3$ (1.2)	2	22 h	r.t.	**18a** (<5)	**19** (**19**)	**20a** (13); **20b** (15)
11	DCM	$In(OTf)_3$ (1.2)	2	22 h	r.t.	**18a** (<5); **18b** (5)	**19** (23)	[b]
12 [c]	DCM	$Sc(OTf)_3$ (1.2)	2	22 h	r.t.	/	/	/
13	DCM	$ZnCl_2$ (0.1)	2	22 h	r.t.	**18a** (<5); **18b** (10)	-	**20a** (44); **20b** (20)
14	DCM	$ZnCl_2$ (0.1)	2	22 h	40	**18a** (6); **18b** (13)	-	**20a** (47); **20b** (21)
15	DCM	ZnI_2 (0.1)	2	22 h	40	**18a** (11); **18b** (10)	-	**20a** (46); **20b** (21)
16	DCM	$ZnBr_2$ (0.1)	2	22 h	40	**18a** (6); **18b** (12)	-	**20a** (45); **20b** (**19**)
17 [d]	DCM	$Zn(OTf)_2$ (0.1)	2	22 h	40	**18a** (<5); **18b** (<5)	-	**20a** (32); **20b** (16)
18	DCM	$ZnCl_2$ (0.1)	2	95 h	40	**18a** (7); **18b** (14)	-	**20a** (31); **20b** (12)
19	DCM	ZnI_2 (0.1)	2	95 h	40	**18a** (12); **18b** (13)	-	**20a** (26); **20b** (9)
20	ACN	$ZnCl_2$ (0.1)	2	22 h	r.t.	**18a** (9); **18b** (8)	-	**20a** (36); **20b** (15)
21	EtOAc	$ZnCl_2$ (0.1)	2	22 h	r.t.	**18a** (5); **18b** (12)	-	**20a** (43); **20b** (22)
22	CH_3NO_2	$ZnCl_2$ (0.1)	2	22 h	r.t.	**18a** (15); **18b** (12)	-	**20a** (41); **20b** (23)
23	DMF	$ZnCl_2$ (0.1)	2	22 h	r.t.	**18a** (<5); **18b** (6)	-	**20a** (36); **20b** (32)
24	ACN	ZnI_2 (0.1)	2	22 h	r.t.	**18a** (11); **18b** (7)	-	**20a** (52); **20b** (17)
25	EtOAc	ZnI_2 (0.1)	2	22 h	r.t.	**18a** (8); **18b** (9)	-	**20a** (56); **20b** (21)
26	CH_3NO_2	ZnI_2 (0.1)	2	22 h	r.t.	**18a** (17); **18b** (9)	-	**20a** (43); **20b** (22)
27	DMF	ZnI_2 (0.1)	2	22 h	r.t.	**18a** (<5); **18b** (<5)	-	[b]
28	DMSO	ZnI_2 (0.1)	2	22 h	r.t.	**18a** (<5); **18b** (<5)	-	**20a** (49); **20b** (27)
29	CH_3NO_2	ZnI_2 (0.1)	2	7 d	r.t.	**18a** (16); **18b** (10)	**19** (<5)	**20a** (24); **20b** (9)
30 [d]	CH_3NO_2	ZnI_2 (0.1)	2	116 h	40	**18a** (15); **18b** (12)	**19**(<5)	**20a** (7)
31 [d]	CH_3NO_2	ZnI_2 (0.1)	2	9 h	80	**18a** (12); **18b** (10)	**19** (8)	**20a** (6); **20b** (<5)
32 [d]	CH_3NO_2	ZnI_2 (0.5)	2	22 h	r.t.	**18a** (5); **18b** (8)	**19** (<5)	**20a** (17); **20b** (<5)
33 [d]	CH_3NO_2	ZnI_2 (1)	2	22 h	r.t.	**18a** (6); **18b** (9)	**19** (15)	-
34 [d]	DCE	ZnI_2 (0.1)	1	48 h	80	**18a** (<5); **18b** (6)	**19** (<5)	**20a** (<5)
35 [d]	DCE	ZnI_2 (0.1)	2	48 h	80	**18a** (7); **18b** (9)	**19** (<5)	**20a** (<5); **20b** (<5)

Standard reaction conditions: Enaminoester **15** (1 mmol), quinone **17**, solvent (4 mL), stirred at specified temperature for specified time; [a] NMR yield; [b] Peak overlap on qNMR; [c] No qNMR was performed, products were isolated by flash column chromatography; [d] Benzofuranone **20a** present in reaction mixture.

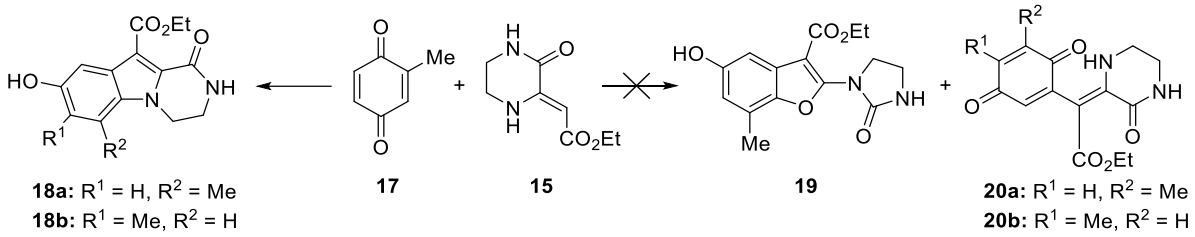

Scheme 4. Aim of this work, promoting the reaction of enamine **15** and quinone **17** towards indole **18a/b**.

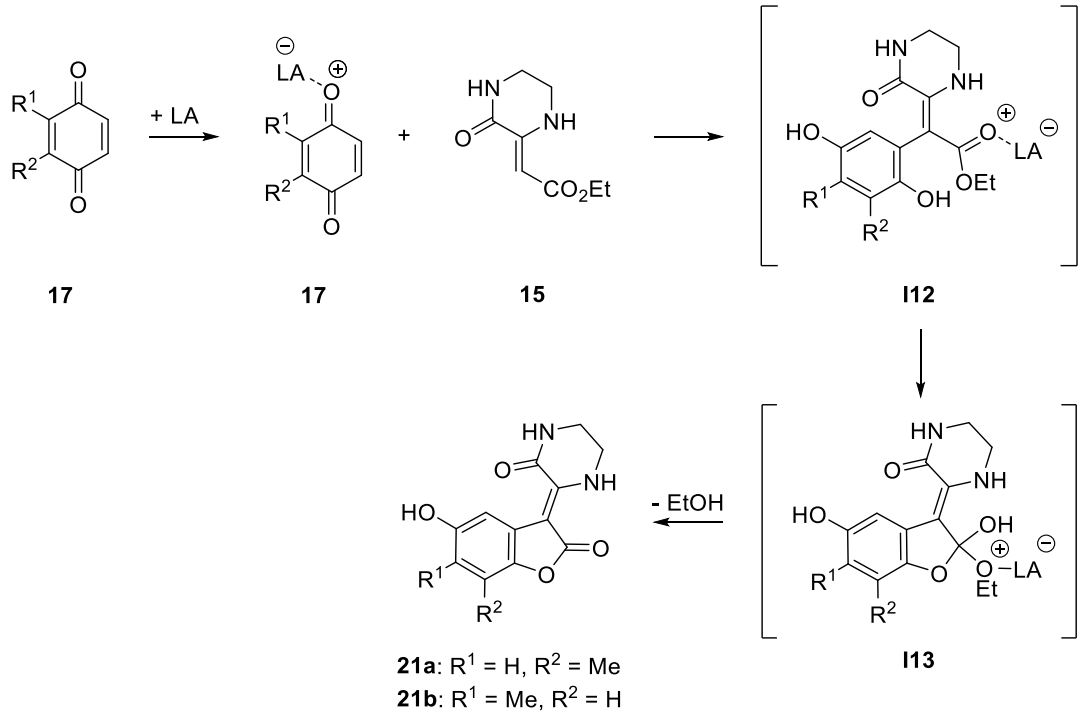

Scheme 5. Proposed reaction mechanism for benzofuranone formation.

Table 2. Multivariate screening of reaction conditions, optimization towards benzofuranones **21a/b**.

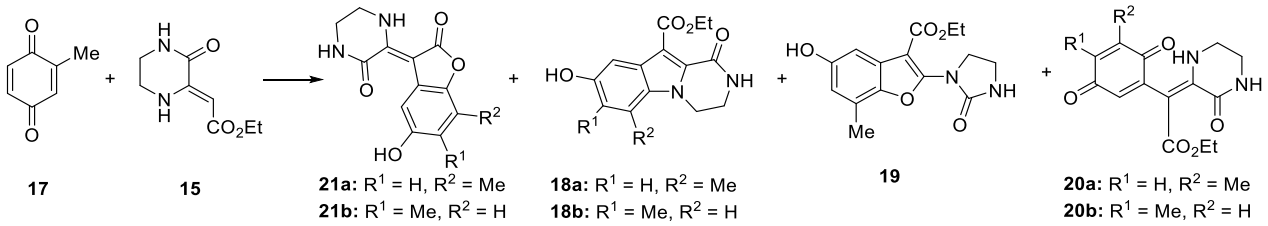

Entry	Solvent	Additive	SM 17 (eq.)	T (°C)	Yield [a] (%)			
					21a/b	18a/b	19	20a/b
36	DCM	$Sc(OTf)_3$	2	r.t.	**21a** (<5)	**18a** (6); **18b** (<5)	-	**20a** (51); **20b** (14)
37	CH_3NO_2	$Sc(OTf)_3$	2	r.t.	**21a** (<5)	**18a** (8); **18b** (<5)	-	**20a** (33); **20b** [b]
38	DCE	$Sc(OTf)_3$	2	80	**21a/b** (11)	**18a** (7); **18b** (<5)	**19** (<5)	**20a** (15); **20b** (8)
39 [c]	DCE	$Sc(OTf)_3$	1	80	**21a/b** (22)	**18a** (6); **18b** (<5)	-	**20a** (<5); **20b** (<5)
40 [c]	DCE	$Zn(OTf)_2$	1	80	**21a/b** (22)	**18a** (<5); **18b** (<5)	-	**20a** (<5)

Standard reaction conditions: Enaminoester **15** (1 mmol), quinone **17**, additive (0.1 mmol), solvent (4 mL), stirred at specified temperature for 22 h. [a] NMR yield; [b] Peak overlap on qNMR; [c] Significant amount of starting material present after 22 h.

Considering the proposed mechanism, we hypothesized that an excess of methyl-*p*-benzoquinone might be disadvantageous since it would promote the oxidation of key

intermediate **I12**. In agreement with this hypothesis, lowering the equivalents of methyl-*p*-benzoquinone from 2 to 1 doubled the combined benzofuranone **21a/b** yield (Table 2). Yields were further improved by increasing the reaction temperature from room temperature to 80 °C. Nevertheless, regioisomeric mixtures of benzofuranones **21a/b** were formed with a combined yield of only 22%, alongside traces of 5-hydroxyindoles **18a/b** and enamino quinones **20a/b**. Interestingly, replacing scandium triflate with zinc triflate had no significant impact on benzofuranone formation. We further hypothesized that the nature of the ester might have an influence on the lactonization step. Therefore, methyl ester derivative **22** was evaluated under the optimized reaction conditions for benzofuranone formation (Scheme 6). Interestingly, the change in ester alkoxy group increased the NMR yield from 22% to 33%, which can be explained by two reasons. Firstly, the lower steric hindrance of the methyl group favors lactonization. Secondly, the slightly lower pKa of methanol compared to ethanol makes the methoxy group a better leaving group.

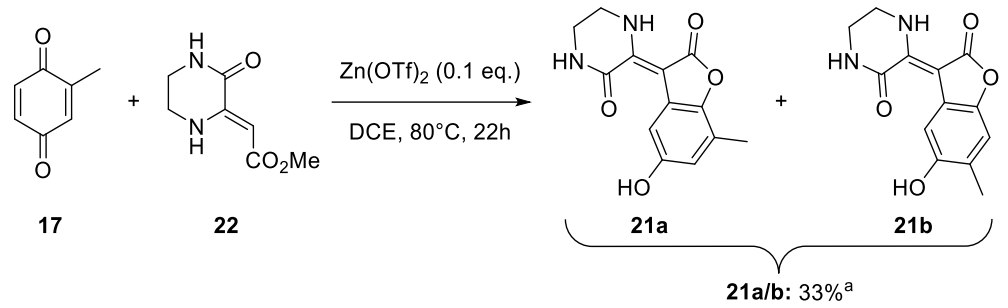

Scheme 6. The reaction of piperazinone enaminoester **22** under optimized reaction conditions for benzofuranone formation. [a] NMR yield.

To evaluate the impact of the enamine starting material, analogues of enaminoester **15** (Figure 1) were evaluated under optimized conditions for 5-hydroxyindole formation. To circumvent the regioselectivity issues, the reaction was performed with unsubstituted p-benzoquinone **1** instead of methyl-p-benzoquinone **17**.

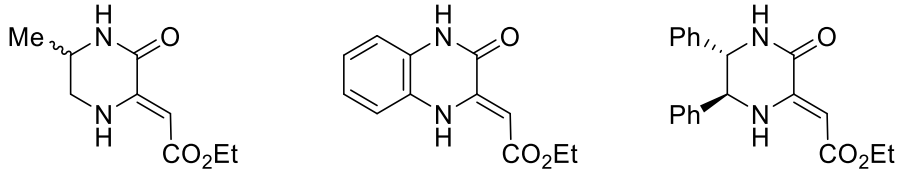

Figure 1. Overview of the evaluated enamines.

Interestingly, the ZnI_2-mediated condensation of enamine **23** and *p*-benzoquinone resulted in the formation of a novel product, which was confirmed to be pyrrolo[2,3-*f*]indole **26** by X-ray diffraction, in addition to small quantities of the corresponding 5-hydroxyindole (Scheme 7). The formation of pyrrolo[2,3-*f*]indoles as (side) products of the Nenitzescu reaction has received little attention in the literature since its first description by Kuckländer in 1973 [39]. Kuckländer obtained small quantities of pyrrolo[2,3-*f*]indoles from the reaction of *N*-substituted enaminoesters with *p*-benzoquinone and proposed that their formation occurs by the addition of a second enamine to enamino quinone intermediate **I2** followed by cyclization and aromatization [39,42]. This mechanism might explain why pyrrolo[2,3-*f*]indoles were not observed in any of the condensation reactions of methyl-*p*-benzoquinone with enamine **15**, since the addition of a second enamine is sterically inhibited by the presence of the methyl substituent.

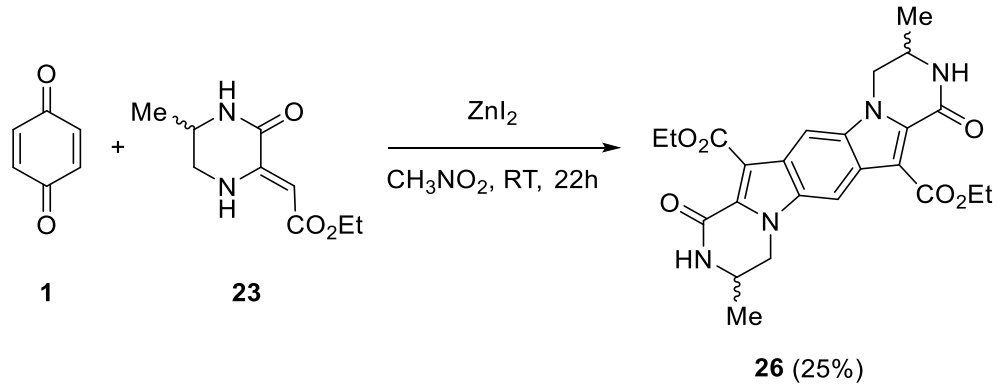

Scheme 7. Formation of a pyrrolo[2,3-*f*]indole.

The reactions of benzoquinone with enamines **24** and **25** were troublesome. Enamine **24** was insoluble in nitromethane, and the reaction resulted in various insoluble products. Heating the reaction mixture to 70 °C resolved the solubility issues yet resulted in the formation of an intractable reaction mixture and decomposition products. Similarly, the reaction of enamine **25** afforded a complex mixture.

The reaction of *p*-benzoquinone with enaminoester **15** was also evaluated under optimized conditions for benzofuranone formation (Scheme 8). The expected 5-hydroxybenzofuranone could not be isolated successfully due to significant side product formation. However, the 5-hydroxyindole **27** could be isolated in a low 9% yield.

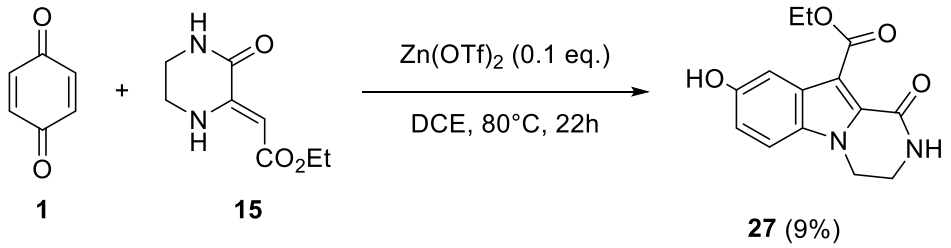

Scheme 8. Reaction of enamine **15** and *p*-benzoquinone under optimized conditions for benzofuranone formation.

3. Conclusions

In conclusion, we further explored the Nenitzescu reaction of piperazinone enaminoesters **15** and **22–25** with methyl-*p*-benzoquinone and *p*-benzoquinone. An extensive screening of reaction conditions led to valuable and new insights into the parameters that influence the condensation of methyl-*p*-benzoquinone and enamine **15**. Zinc halides ($ZnBr_2$, $ZnCl_2$ or ZnI_2) promoted 5-hydroxyindole formation most efficiently, and surprisingly the halide counterion affected the regioselectivity significantly. Besides the acid mediator, the solvent also influenced the regio- and chemoselectivity, and nitromethane was found to be the most suitable for indole formation. In addition to 5-hydroxyindoles, benzofurans and enamino quinones, we observed novel reaction products that are rarely described in the literature: benzofuranones **21a/b**. A limited optimization study allowed for substantiating the proposed reaction mechanism and simultaneously increasing the yield. Nevertheless, finding selective and generally applicable reaction conditions proved to be challenging. Besides benzofuranones, another novel product was formed, namely pyrrolo[2,3-*f*]indole **26**. This product was only observed in the condensation of *p*-benzoquinone with enamine **23**.

4. Experimental Section

4.1. Materials and Methods

All reagents were purchased from Acros Organics (Geel, Belgium), Alfa Aesar (Kandel, Germany), Fluorochem (Hadfield, UK), Merck (Darm-stadt, Germany) or TCI Europe

(Zwijndrecht, Belgium) and used as received. All reactions were performed in screw-capped reaction tubes, using aluminum heating blocks and magnetic stirring. The reaction was monitored by TLC analysis with Macherey-Nagel SILPre-coated ALUGRAM® Xtra SIL G/UV254 TLC sheets or MilliporeSigmaTM Silica Gel 60 F254 Coated Aluminum-Backed TLC Sheets. Compounds were visualized under UV irradiation (254 nm), visible light or with iodine coated silica. Column chromatography was performed manually with silica 60, 70–230 mesh (Acros, Geel, Belgium) as the stationary phase or with a CombiFlash EZ prep apparatus using BGB Scorpius Silica 60 Å Irregular—50 mm cartridges. Solvents were concentrated under vacuum with a rotary evaporator at 50 °C.

Methyl-benzoquinone and *p*-benzoquinone slowly decompose over time and should be stored in a sealed vessel, refrigerated, and in the dark [50]. The quality of the quinone was evaluated visually and by ^{1}H NMR. In the case of an insufficient purity (<95%), the quinone was sublimated according to the literature procedure [50].

^{1}H NMR and ^{13}C NMR spectra were recorded on a Bruker Avance 400 (400 MHz working frequency). Samples were prepared in $CDCl_3$ or DMSO-d_6, and chemical shifts (δ) were reported in parts per million (ppm) with reference to tetramethylsilane ($CDCl_3$) or the internal (NMR) solvent signal (DMSO-d_6) [51]. High-resolution mass spectra (HRMS) were measured on a quadrupole orthogonal acceleration time-of-flight mass spectrometer (Synapt G2 HDMS, Waters, Milford, MA, USA) with an infusion rate of 3 mL/min and a resolution of 15,000 (FWHMdfull width at half maximum). Spectra were obtained in positive ionization mode with leucine enkephalin as a lock mass.

Melting points were measured on a Reichert Thermovar apparatus and are uncorrected.

Yellow single crystals of pyrrolo[2,3-*f*]indole **26** suitable for X-ray diffraction were obtained by recrystallization in DMSO. X-ray intensity data were collected at 293(2) K on an Agilent SuperNova diffractometer with monochromated Mo-K_α radiation (λ = 0.71073 Å). The images were interpreted and integrated with CrysAlisPRO [52] and the implemented absorption correction was applied. The structure was solved using Olex2 [53] with the ShelXT [54] structure solution program using Intrinsic Phasing and refined with the ShelXL [55] refinement package using full-matrix least-squares minimization on F^2. Non-hydrogen atoms were refined anisotropically and hydrogen atoms in the riding mode with isotropic temperature factors were fixed at 1.2 times the U_{eq} of the parent atoms (1.5 times U_{eq} for methyl groups). Hydrogen atom H1 attached to N1 was located in a difference electron density map and subsequently freely refined. The asymmetric unit consisted of half a molecule and one molecule of DMSO. The whole molecule was generated by inversion symmetry. Atom C2 (flap of piperazine ring) and atoms C15 and C16 (ethoxy group) were found to be disordered over two positions, with occupancies of 0.518(17):0.482(17) for C2 and 0.62(3):0.38(3) for C15, C16. The structure was refined as a two-component twin (BASF = 0.289). Olex2 [53] was used for the structure presentation in Figure 2.

The crystal data for compound **26**: $C_{28}H_{38}N_4O_8S_2$, M = 662.74 g/mol, monoclinic system, space group *I*2/*a*, *a* = 8.6600(6) Å, *b* = 14.0356(8) Å, *c* = 26.3917(17) Å, β = 98.638(7)°, *Z* = 4, *V* = 3171.5(4) Å^3, D_c = 1.304 g cm^{-3}, μ(MoK_α) = 0.220 mm^{-1}, *T* = 293(2) K, 5283 independent reflections, and crystal dimensions of 0.50 × 0.10 × 0.10 mm^3. The final R_1 was 0.0667 (I > 2σ(I)) and wR_2 was 0.1932 (all data).

The crystallographic data for the structure reported in this paper have been deposited with the Cambridge Crystallographic Data Centre. Copies of the data (CCDC registration number 2236215) can be obtained from the CCDC free of charge by sending an application to the following e-mail address: deposit@ccdc.cam.ac.uk.

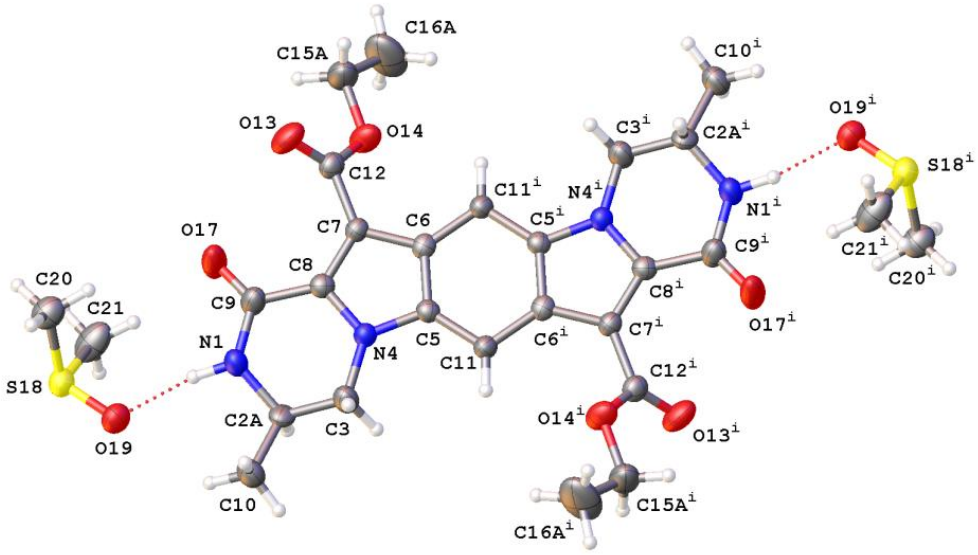

Figure 2. Crystal structure of compound **26**. Thermal ellipsoids are drawn at the 30% probability level. H atoms are shown as small circles of arbitrary radii. For the disordered moieties, only the major conformation is shown. Symmetry code: (i) 1—*x*, 1—*y*, 1—*z*.

4.2. Synthesis of Piperazinone Enaminoesters

General procedure: Piperazinone enaminoesters **15**, **22–25** were prepared according to a modified literature procedure [23]. To a flame-dried, nitrogen-flushed round bottom two-necked flask equipped with a stir bar, 1,2-diamine (20 mmol, 1.00 eq.) and ethanol (8.0 mL) were added. To the stirred solution at room temperature, a solution of diethyl acetylenedicarboxylate (DEAD) or dimethyl acetylenedicarboxylate (DMAD) (20 mmol, 1.00 eq.) in 8.0 mL ethanol was added dropwise (0.3 mL/min) using a syringe pump. After stirring for three hours at room temperature, during which the product crystallized from the reaction mixture, the mixture was vacuum filtered. The obtained solid was washed with small amounts of diethyl ether and dried under vacuum to afford the products as crystalline solids.

Ethyl (*Z*)-2-(3-oxopiperazin-2-ylidene)acetate **(15)** (see Supplementary Materials).

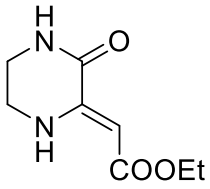

Prepared according to the general procedure, using ethylenediamine (1.209 g, 20.12 mmol, 1.00 eq.) and DEAD (3.424 g, 20.12 mmol, 1.00 eq.), product **15** was obtained as a crystalline white solid (2.353 g, 12.78 mmol, 64%).

Alternatively, product **15** was prepared according to a slightly adapted procedure, using ethylenediamine (0.608 g, 10.12 mmol, 1.00 eq.) and DEAD (1.723 g, 10.13 mmol, 1.00 eq.), each dissolved in 4.0 mL of ethanol. The reaction was performed in oven-dried flasks in an air atmosphere instead of an inert atmosphere. Product **15** was isolated as a crystalline white solid (0.998 g, 5.418 mmol, 54%).

For the large-scale preparation, on a 180 mmol scale, the general procedure was slightly adapted. Instead of a syringe pump, an addition funnel in an argon atmosphere was used to add the DEAD ethanol solution. Ethylenediamine (10.931 g, 181.88 mmol, 1.03 eq.) and DEAD (30.158 g, 177.23 mmol, 1.00 eq.) were each dissolved in 80.0 mL ethanol. Product **15** was isolated as a crystalline white solid (19.124 g, 103.83 mmol, 59%). ^{1}H NMR (400 MHz, $CDCl_3$), δ 8.28 (s, 1H), 6.65 (s, 1H), 5.63 (s, 1H), 4.15 (q, *J* = 7.1 Hz, 2H), 3.55–3.49 (m, 2H), 3.45–3.40 (m, 2H), 1.27 (t, *J* = 7.1 Hz, 3H). ^{1}H NMR corresponds with literature reports [43].

Methyl (*Z*)-2-(3-oxopiperazin-2-ylidene)acetate **(22)**.

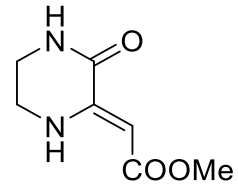

Prepared with small alterations to the general procedure using ethylenediamine (0.607 g, 10.10 mmol, 1.01 eq.) and DMAD (1.421 g, 10.00 mmol, 1.00 eq.), each were dissolved in 4.0 mL methanol instead of ethanol. Product **22** was obtained as a crystalline off-white solid (1.137 g, 6.68 mmol, 67%). ^{1}H NMR (400 MHz, $CDCl_3$) δ 8.28 (s, 1H), 6.61 (s, 1H), 5.63 (s, 1H), 3.69 (s, 3H), 3.55–3.49 (m, 2H), 3.45–3.40 (m, 2H). ^{1}H NMR corresponds with literature reports [56].

Ethyl (*Z*)-2-(5-methyl-3-oxopiperazin-2-ylidene)acetate **(23)**.

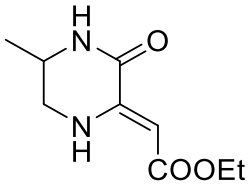

Prepared according to the general procedure, using 1,2-diaminopropane (racemic mixture, 741 mg, 10.0 mmol, 1.10 eq.) and DEAD (1.549 g, 9.106 mmol, 1.00 eq.). Product **23** was obtained as a crystalline white solid (628 mg, 3.17 mmol, 35%). ^{1}H NMR (300 MHz, $CDCl_3$) δ 8.24 (br. s, 1H), 6.45 (br. s, 1H), 5.63 (s, 1H), 4.15 (q, *J* = 7.1 Hz, 2H), 3.86–3.75 (m, 1H), 3.43–3.36 (m, 1H), 3.16–3.08 (m, 1H), 1.31–1.23 (m, 6H). ^{1}H NMR corresponds with literature reports [43].

Ethyl (Z)-2-(3-oxo-3,4-dihydroquinoxalin-2(1H)-ylidene)acetate **(24)**.

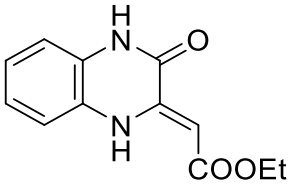

Prepared according to the general procedure, using 1,2-phenylenediamine (1.081 g, 9.996 mmol, 1.02 eq.) and DEAD (1.734 g, 10.19 mmol, 1.00 eq.). A crystalline yellow solid containing **24** and its imine isomer were obtained in a 1:0.25 ratio (1.793 g, 7.720 mmol, 77%). ^{1}H NMR (400 MHz, DMSO-d_6) δ 11.72 (s, 1H), 11.06 (s, 1H), 7.42–7.38 (m, 1H), 7.08–6.98 (m, 3H), 5.50 (s, 1H), 4.16 (q, *J* = 7.1 Hz, 2H), 1.24 (t, *J* = 7.1 Hz, 3H). Imine-isomer: ^{1}H NMR (400 MHz, DMSO-d_6) δ 12.48 (s, 1H), 7.78–7.72 (m, 1H), 7.57–7.50 (m, 1H), 7.33–7.28 (m, 2H), 4.10 (q, *J* = 7.1 Hz, 2H), 3.81 (s, 2H), 1.18 (t, *J* = 7.1 Hz, 3H). ^{1}H NMR corresponds with literature reports [43].

Ethyl (Z)-2-((5S,6S)-3-oxo-5,6-diphenylpiperazin-2-ylidene)acetate **(25)**.

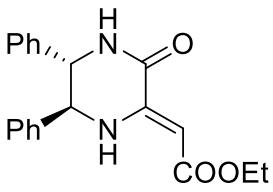

Prepared according to a modified version of the general procedure using (1*S*,2*S*)-1,2-diphenylethylenediamine (2.125 mg, 10.01 mmol, 1.00 eq.), and DEAD (1.702 g, 10.00 mmol,

1.00 eq.). The reaction mixture was stirred for 20 h, dried, and dissolved in DCM, then filtered over silica using petroleum ether and dried under reduced pressure. Product **25** was obtained as a crystalline white solid (2.962 g, 8.805 mmol, 88%). ^{1}H NMR (400 MHz, $CDCl_3$) δ 8.43 (s, 1H), 7.29–7.19 (m, 6H), 7.12–7.03 (m, 4H), 6.19 (s, 1H), 5.83 (s, 1H), 4.69 (d, J = 9.4 Hz, 1H), 4.53 (d, J = 9.5 Hz, 1H), 4.14 (qd, J = 7.1, 1.0 Hz, 2H), 1.28 (t, J = 7.1 Hz, 3H). ^{1}H NMR corresponds with literature reports [43].

4.3. qNMR Optimization Study

General procedure: To a flame-dried, nitrogen-flushed reaction tube equipped with a stir bar, piperazinone enaminoester **15** (184 mg, 1.00 mmol, 1.00 eq.), methyl-*p*-benzoquinone (244 mg, 2.00 mmol, 2.00 eq.), the appropriate (dry) solvent (4.0 mL) and if applicable, a solid additive, were added. If applicable, the appropriate liquid additive was added dropwise to the stirred mixture cooled to 0 °C in an ice bath. After stirring the reaction mixture at room temperature for 30 min, and at the reaction temperature for the appropriate time, the solution was cooled to room temperature, quenched with $NaHCO_3$ (20 mL) and water (30 mL), diluted with ethyl acetate (50 mL) and extracted three times with ethyl acetate (3 × 50 mL). The combined organic phases were washed with water (3 × 50 mL) and brine (1 × 50 mL), and dried over Na_2SO_4. Benzyl benzoate (140 µL, 0.66 mmol) and DMSO-d_6 (1 mL) were added to the crude mixture, and 0.10 mL of the homogeneous solution was diluted to 0.50 mL with DMSO-d_6 and analyzed by ^{1}H NMR.

qNMR yield determination: The product yields were determined by the following equation:

$$Yield(\%) = \frac{I_{Analyte}}{I_{IS}} * \frac{n_{IS}}{n_{SM}} * \frac{N_{IS}}{N_{Analyte}} * 100$$

With $I_{Analyte}$: integral of the analyte signal, I_{IS}: integral of the internal standard signal, n_{IS}: number of moles of the internal standard, n_{SM}: number of moles of the starting material, N_{IS}: number of protons responsible for the internal standard signal, $N_{Analyte}$: number of protons responsible for the analyte signal.

4.4. Synthesis of Reaction Products

Ethyl 5-hydroxy-7-methyl-2-(2-oxoimidazolidin-1-yl)benzofuran-3-carboxylate **(19)**.

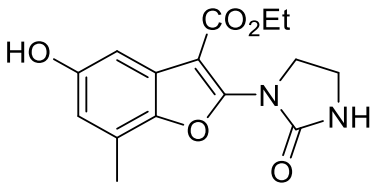

Prepared according to a literature procedure [23,43]. To a flame-dried, nitrogen-flushed round-bottom flask equipped with a stirring bar, piperazinone enaminoester **15** (92 mg, 0.50 mmol, 1.0 eq.), methyl-*p*-benzoquinone (126 mg, 1.03 mmol, 2.07 eq.) and dry acetonitrile (2.0 mL) were added. The mixture was stirred and cooled to 0 °C in an ice bath. Subsequently, 48% $BF_3{\cdot}OEt_2$ (0.62 mmol, 76 µL, 1.2 eq.) was added dropwise using a Hamilton microsyringe. After stirring at room temperature for three hours, the solution was diluted with ethyl acetate (50 mL) and water (50 mL) and extracted with ethyl acetate (3 × 50 mL). The combined organic phases were washed with water (3 × 50 mL) and brine (1 × 50 mL), and dried over Na_2SO_4, coated on celite and purified using flash column chromatography (ethyl acetate:isohexane) to afford **19** as a brown solid (84 mg, 0.28 mmol, 55%). ^{1}H NMR (400 MHz, DMSO-d_6) δ 9.25 (s, 1H), 7.33 (s, 1H), 7.06 (dd, J = 0.4 Hz, J = 2.5 Hz, 1H), 6.60 (dd, J = 0.8 Hz, J = 2.5 Hz, 1H), 4.24 (q, J = 7.2 Hz, 2H), 3.99–3.93 (m, 2H), 3.53–3.46 (m, 2H), 2.33–2.36 (m, 3H), 1.31 (t, J = 7.2 Hz, 2H). ^{1}H NMR corresponds with literature reports [43].

Ethyl-2-(5-methyl-3,6-dioxocyclohexa-1,4-dien-1-yl)-2-(3-oxopiperazin-2-ylidene)acetate **(20a)** and ethyl-2-(4-methyl-3,6-dioxocyclohexa-1,4-dien-1-yl)-2-(3-oxopiperazin-2-ylidene)acetate **(20b)**.

Prepared according to a modified literature procedure [57]. To a flame-dried, nitrogen-flushed reaction tube equipped with stir bar, enaminoester **15** (184 mg, 1.00 mmol, 1.00 eq.) and nitromethane (2.0 mL) were added. A solution of methyl-*p*-benzoquinone (244 mg, 2.00 mmol, 2.00 eq.) in nitromethane (1.0 mL) was added to the mixture and stirred at room temperature overnight, and at 60 °C for three hours. The reaction mixture was coated on celite and purified by flash column chromatography (ethyl acetate: isohexane) to obtain a regioisomeric mixture of **20a** and **20b** (272 mg, 0.894 mmol, 89%).

Ethyl-2-(5-methyl-3,6-dioxocyclohexa-1,4-dien-1-yl)-2-(3-oxopiperazin-2-ylidene)acetate (**20a**):

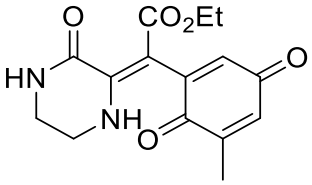

Part of the regioisomeric mixture (50 mg, 0.16 mmol) was dissolved in DCM (2 mL) and purified by HPLC (ethyl acetate: isohexane). Product **20a** was obtained as a red solid; Mp: 75 °C-80 °C. ^{1}H NMR (400 MHz, DMSO-d_6) δ 9.69–9.57 (m, 1H), 8.68–8.58 (m, 1H), 6.67–6.59 (m, 1H), 6.35 (d, J = 2.7 Hz, 1H), 4.13–4.00 (m, 2H), 3.43 (br. s, 2H), 3.31–3.28 (m, 2H), 1.94 (d, J = 1.5 Hz, 3H), 1.11 (t, J = 7.1 Hz).^{13}C{^{1}H} NMR (101 MHz, DMSO-d_6) δ 188.1, 187.4, 168.4, 160.5, 151.0, 148.1, 146.8, 133.2, 130.4, 90.6, 59.9, 39.9, 39.2, 16.2, 14.7 HRMS (ESI-Q-TOF): m/z [M+H]$^{+}$ calcd. for $C_{15}H_{16}N_2O_5$: 305.1132; found: 305.1131.

Ethyl-2-(4-methyl-3,6-dioxocyclohexa-1,4-dien-1-yl)-2-(3-oxopiperazin-2-ylidene)acetate (**20b**):

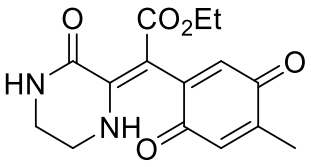

Part of the regioisomeric mixture (100 mg, 0.330 mmol) was dissolved in DCM (2 mL) and purified by HPLC (isopropanol: dichloromethane). Product **20b** was obtained as a red solid (10 mg, 0.033 mmol); Mp: 80–85 °C. ^{1}H NMR (400 MHz, DMSO-d_6) δ 9.68–9.62 (m, 1H), 8.60–8.55 (m, 1H), 6.68 (q, J = 1.6 Hz, 1H), 6.42 (s, 1H), 4.05 (q, J = 7.0 Hz, 2H), 3.43 (br. s, 2H), 3.31–3.28 (m, 2H), 1.96 (d, J = 1.6 Hz, 3H), 1.12 (t, J = 7.0 Hz, 3H). ^{13}C{^{1}H} NMR (101 MHz, DMSO-d_6) δ 188.4, 187.2, 168.4, 160.5, 151.6, 147.6, 145.5, 134.3, 130.5, 89.9, 59.8, 40.0, 39.2, 15.5, 14.7. HRMS (ESI-Q-TOF): m/z [M+H]$^{+}$ calcd. for $C_{15}H_{16}N_2O_5$: 305.1132; found: 305.1129.

Ethyl 8-hydroxy-1-oxo-1,2,3,4-tetrahydropyrazino[1,2-a]indole-10-carboxylate **(27)**.

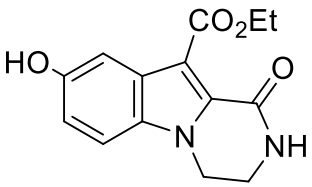

To a flame-dried, nitrogen-flushed reaction tube equipped with a stir bar, piperazinone enaminoester **15** (184 mg, 1.00 mmol, 1.00 eq.), *p*-benzoquinone (108 mg, 1.00 mmol, 1.00 eq.), DCE (4.0 mL), and Zn(OTf)$_2$ (36 mg, 0.10 mmol, 0.10 eq.) were added. After stirring the reaction at room temperature for half an hour, and at 80 °C for 22 h, the solution

was cooled to room temperature, quenched with $NaHCO_3$ (0.2 mL) and water (10 mL), diluted with ethyl acetate (20 mL) and extracted with ethyl acetate (3 × 20 mL). The combined organic phases were washed with water (3 × 10 mL) and brine (1 × 10 mL), and dried over Na_2SO_4, coated on celite and purified by flash column chromatography (MeOH: DCM). Product **26** was obtained as a yellow solid (25 mg, 0.091 mmol, 9%); Mp: 110–115 °C. ^{1}H NMR (400 MHz, DMSO-d_6) δ 9.22 (s, 1H), 8.26 (s, 1H), 7.43 (d, *J* = 9.0 Hz, 1H), 7.22 (d, *J* = 1.9 Hz, 1H), 6.88 (dd, *J* = 2.1 Hz, *J* = 8.9 Hz, 1H), 4.17–4.34 (m, 4H), 3.54–3.64 (m, 2H), 1.31 (t, *J* = 7.1 Hz, 3H). ^{13}C{^{1}H} NMR (101 MHz, DMSO-d_6) δ 164.4, 158.5, 153.5, 130.7, 129.7, 127.2, 116.2, 112.4, 108.4, 104.8, 60.12, 41.4, 39.4, 14.7. HRMS (ESI-Q-TOF): m/z $[M+H]^+$ calcd. for $C_{14}H_{14}N_2O_4$: 275.1026; found: 275.1031.

Ethyl 8-hydroxy-6-methyl-1-oxo-1,2,3,4-tetrahydropyrazino[1,2-*a*]indole-10-carboxylate **(18b)** and ethyl 8-hydroxy-7-methyl-1-oxo-1,2,3,4-tetrahydropyrazino[1,2-*a*]indole-10-carboxylate **(18a)**.

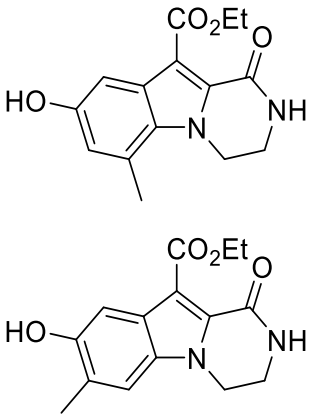

Prepared according to a modified literature procedure [43]. To a flame-dried, nitrogen-flushed reaction tube equipped with a stir bar, piperazinone enaminoester **15** (92 mg, 0.50 mmol, 1.00 eq.), methyl-*p*-benzoquinone (122 mg, 1.00 mmol, 2.00 eq.) and dry diethyl ether (2.0 mL) were added. The reaction was stirred and cooled to 0 °C in an ice bath and 48% $BF_3{\cdot}OEt_2$ (0.62 mmol, 76 µL, 1.2 eq.) was added dropwise using a Hamilton microsyringe. After stirring at room temperature for 1 h, and at 40 °C overnight, the reaction mixture was vacuum filtered, washed with small amounts of Et_2O and dried under vacuum. The crude solid was coated on celite and purified by flash column chromatography (methanol: dichloromethane) to afford a regioisomeric mixture containing **18a** and **18b** in a 7:2 ratio (26 mg, 0.091 mmol, 18%). Due to the very low solubility of the regioisomers, no further separation was performed. ^{1}H NMR (400 MHz, DMSO-d_6) Regioisomer **18a** *δ* 9.08 (br. s, 1H), 8.22–8.27 (m, 1H), 6.98 (d, *J* = 2.3 Hz, 1H), 6.60 (dd, *J* = 0.8 Hz, *J* = 2.3 Hz, 1H), 4.56–4.51 (m, 2H), 4.24 (q, *J* = 7.1 Hz, 2H), 3.61–3.53 (m, 2H), 2.63 (br. s, 3H), 1.29 (t, *J* = 7.2 Hz, 3H) Regioisomer **18b** *δ* 9.26 (br. s, 1H), 8.19 (1H), 7.31 (s, 1H), 7.25 (s, 1H), 4.17–4.22 (m, 2H), 4.24 (q, *J* = 7.1 Hz, 2H), 3.61–3.53 (m, 2H), 2.26 (br. s, 3H), 1.30–1.36 (m, 3H). HRMS (ESI-Q-TOF): m/z $[M+H]^+$ calcd. for $C_{15}H_{16}N_2O_4$: 289.1183; found: 289.1180.

(*Z*)-3-(5-Hydroxy-7-methyl-2-oxobenzofuran-3(2H)-ylidene)piperazin-2-one **(21a)**.

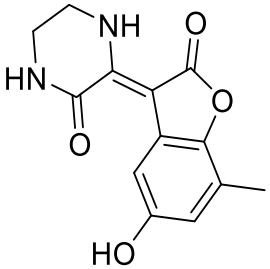

To a flame-dried, nitrogen-flushed reaction tube equipped with a stir bar, piperazinone enaminoester **15** (367 mg, 1.99 mmol, 1.00 eq.), methyl-*p*-benzoquinone (487 mg, 3.99 mmol,

2.00 eq.), dry DCM (8.0 mL), and $Sc(OTf)_3$ (101 mg, 0.205 mmol, 0.10 eq.) were added. After stirring at 40 °C for 22 h, the solution was cooled to room temperature, quenched with $NaHCO_3$ (20 mL) and water (30 mL), diluted with ethyl acetate (50 mL) and extracted with ethyl acetate (3 × 50 mL). The combined organic phases were washed with water (3 × 50 mL) and brine (1 × 50 mL), and dried over Na_2SO_4, coated on celite and purified by column chromatography (MeOH: Et_2O). Product **21a** was obtained as a yellow solid (16 mg, 0.061 mmol, 3.1%); Mp: >300 °C. ^{1}H NMR (400 MHz, DMSO-d_6) δ 10.14–10.04 (m, 1H), 8.94–8.86 (m, 1H), 8.81 (s, 1H), 7.45 (d, *J* = 2.4 Hz, 1H), 6.34 (d, *J* = 2.1 Hz, 1H), 3.64–3.62 (m, 2H), 3.45–3.36 (m, 2H), 2.17 (s, 3H). ^{13}C{^{1}H} NMR (101 MHz, DMSO-d_6) δ 171.7, 159.2, 152.6, 149.3, 140.9, 124.1, 118.5, 112.8, 107.7, 90.9, 40.3, 38.9, 14.8. HRMS (ESI-Q-TOF): m/z $[M+H]^+$ calcd. for $C_{13}H_{12}N_2O_4$: 261.0870; found: 261.0868.

Diethyl 3,10-dimethyl-1,8-dioxo-1,2,3,4,8,9,10,11-octahydropyrazino[1,2-*a*] pyrazino pyrrolo[2,3-*f*]indole-7,14-dicarboxylate **(26)**.

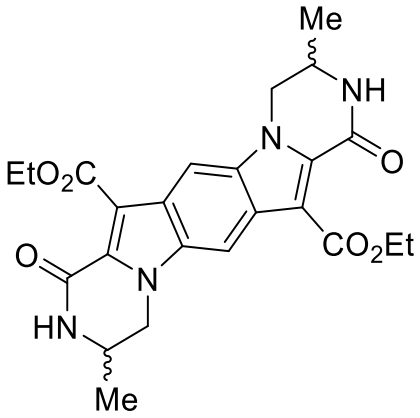

To a flame-dried, nitrogen-flushed reaction tube equipped with a stir bar, piperazinone enaminoester **23** (199 mg, 1.00 mmol, 1.00 eq.), *p*-benzoquinone (216 mg, 2.00 mmol, 2.00 eq.), nitromethane (4 mL), and ZnI_2 (34 mg, 0.11 mmol, 0.11 eq.) were added. After stirring the reaction at room temperature for 22 h, during which the product crystallized from the reaction mixture, the mixture was vacuum filtered. The obtained solid was heated in nitromethane and centrifugated, and the precipitate was dried in vacuum to afford product **26** as a yellow solid (59 mg, 0.13 mmol, 25%); Mp: >300 °C. After recrystallization in DMSO, the product was identified by single-crystal X-ray diffraction (Figure 2). HRMS (ESI-Q-TOF): m/z $[M+H]^+$ calcd. for $C_{24}H_{26}N_4O_6$: 467.1925; found: 467.1927.

Supplementary Materials: The supplementary information containing the NMR spectra can be downloaded at: https://www.mdpi.com/article/10.3390/org4020012/s1.

Author Contributions: R.H. writing—original draft preparation, formal analysis, methodology, data curation; M.V.H. writing—review and editing, conceptualization, validation, supervision; L.V.M. data acquisition and analysis; W.D. conceptualization, supervision, project administration, funding acquisition. All authors have read and agreed to the published version of the manuscript.

Funding: L.V.M. thanks the Hercules Foundation for supporting the purchase of the diffractometer through project AKUL/09/0035. Mass spectrometry was made possible by the support of the Hercules Foundation of the Flemish Government (grant 20100225–7). W.D. acknowledges financial support for this work by the KU Leuven (C14/19/078).

Data Availability Statement: Crystallographic data have been deposited with the Cambridge Crystallographic Data Center (Deposition Number 2236215) and can be obtained free of charge.

Acknowledgments: The authors thank Jez Rozenski for technical assistance with HR-MS measurements and Bart Van Huffel, Gert Steurs and Wim De Borggraeve for technical support with NMR-acquisition.

Conflicts of Interest: The authors declare no conflict of interest. The funders had no role in the design of the study; in the collection, analyses, or interpretation of data; in the writing of the manuscript; or in the decision to publish the results.

References

1. Dumitrascu, F.; Ilies, M.A. Recent Advances in the Nenitzescu Indole Synthesis (1990–2019). *Adv. in Heterocycl. Chem.* **2021**, *133*, 65–177. [CrossRef]
2. Singh, R.; Prakash, R.; Dehaen, W. Polycyclic Heterocycles by Condensation of 1,4-Benzoquinone Analogs and Nucleophiles. *Adv.in Heterocycl. Chem.* **2021**, *135*, 319–410. [CrossRef]
3. Blaising, J.; Polyak, S.J.; Pécheur, E.I. Arbidol as a Broad-Spectrum Antiviral: An Update. *Antiviral Res.* **2014**, *107*, 84–94. [CrossRef] [PubMed]
4. Vigerelli, H.; Sciani, J.M.; Pereira, P.M.C.; Lavezo, A.A.; Silva, A.C.R.; Collaço, R.C.O.; Rocha, T.; Bueno, T.C.; Pimenta, D.C. Bufotenine, a Tryptophan-Derived Alkaloid, Suppresses the Symptoms and Increases the Survival Rate of Rabies-Infected Mice: The Development of a Pharmacological Approach for Rabies Treatment. *J. Venom. Anim. Toxins Incl. Trop. Dis.* **2020**, *26*, e20190050. [CrossRef] [PubMed]
5. Fink, S.L.; Vojtech, L.; Wagoner, J.; Slivinski, N.S.J.; Jackson, K.J.; Wang, R.; Khadka, S.; Luthra, P.; Basler, C.F.; Polyak, S.J. The Antiviral Drug Arbidol Inhibits Zika Virus. *Sci. Rep.* **2018**, *8*, 2–10. [CrossRef]
6. Boriskin, Y.S.; Pécheur, E.I.; Polyak, S.J. Arbidol: A Broad-Spectrum Antiviral That Inhibits Acute and Chronic HCV Infection. *Virol. J.* **2006**, *3*, 56. [CrossRef]
7. Chai, H.; Zhao, Y.; Zhao, C.; Gong, P. Synthesis and In Vitro Anti-Hepatitis B Virus Activities of Some Ethyl 6-Bromo-5-Hydroxy-1H-Indole-3-Carboxylates. *Bioorganic Med. Chem.* **2006**, *14*, 911–917. [CrossRef]
8. Pécheur, E.-I.; Borisevich, V.; Halfmann, P.; Morrey, J.D.; Smee, D.F.; Prichard, M.; Mire, C.E.; Kawaoka, Y.; Geisbert, T.W.; Polyak, S.J. The Synthetic Antiviral Drug Arbidol Inhibits Globally Prevalent Pathogenic Viruses. *J. Virol.* **2016**, *90*, 3086–3092. [CrossRef]
9. Amani, B.; Amani, B.; Zareei, S.; Zareei, M. Efficacy and Safety of Arbidol (Umifenovir) in Patients with COVID-19: A Systematic Review and Meta-Analysis. *Immun. Inflamm. Dis.* **2021**, *9*, 1197–1208. [CrossRef]
10. Zhu, Z.; Lu, Z.; Xu, T.; Chen, C.; Yang, G.; Zha, T.; Lu, J.; Xue, Y. Arbidol Monotherapy Is Superior to Lopinavir/Ritonavir in Treating COVID-19. *J. Infect.* **2020**, *81*, e21–e23. [CrossRef]
11. Lucas, S. The Pharmacology of Indomethacin. *Headache* **2016**, *56*, 436–446. [CrossRef] [PubMed]
12. Fukai, T.; Kaitou, K.; Terada, S. Antimicrobial Activity of 2-Arylbenzofurans from Morus Species against Methicillin-Resistant Staphylococcus Aureus. *Fitoterapia* **2005**, *76*, 708–711. [CrossRef] [PubMed]
13. Tan, Y.X.; Yang, Y.; Zhang, T.; Chen, R.Y.; Yu, D.Q. Bioactive 2-Arylbenzofuran Derivatives from Morus Wittiorum. *Fitoterapia* **2010**, *81*, 742–746. [CrossRef] [PubMed]
14. Zelová, H.; Hanáková, Z.; Čermáková, Z.; Šmejkal, K.; DalÍ Acqua, S.; Babula, P.; Cvačka, J.; Hošek, J. Evaluation of Anti-Inflammatory Activity of Prenylated Substances Isolated from Morus Alba and Morus Nigra. *J. Nat. Prod.* **2014**, *77*, 1297–1303. [CrossRef]
15. Salomé, C.; Narbonne, V.; Ribeiro, N.; Thuaud, F.; Serova, M.; De Gramont, A.; Faivre, S.; Raymond, E.; Désaubry, L. Benzofuran Derivatives as a Novel Class of Inhibitors of MTOR Signaling. *Eur. J. Med. Chem.* **2014**, *74*, 41–49. [CrossRef]
16. Durán, N.; Justo, G.Z.; Ferreira, C.V.; Melo, P.S.; Cordi, L.; Martins, D. Violacein: Properties and Biological Activities. *Biotechnol. Appl. Biochem.* **2007**, *48*, 127. [CrossRef]
17. Salomé, C.; Ribeiro, N.; Chavagnan, T.; Thuaud, F.; Serova, M.; De Gramont, A.; Faivre, S.; Raymond, E.; Désaubry, L. Benzofuran Derivatives as Anticancer Inhibitors of MTOR Signaling. *Eur. J. Med. Chem.* **2014**, *81*, 181–191. [CrossRef]
18. Page, R.L.; Hamad, B.; Kirkpatrick, P. Dronedarone. *Nat. Rev. Drug Discov.* **2009**, *8*, 769–770. [CrossRef]
19. Singh, R.; Horsten, T.; Prakash, R.; Dey, S.; Dehaen, W. Application of the Meerwein Reaction of 1,4-Benzoquinone to a Metal-Free Synthesis of Benzofuropyridine Analogues. *Beilstein J. Org. Chem.* **2021**, *17*, 977–982. [CrossRef]
20. Winant, P.; Dehaen, W. A Visible-Light-Induced, Metal-Free Bis-Arylation of 2,5-Dichlorobenzoquinone. *Beilstein J. Org. Chem.* **2021**, *17*, 2315–2320. [CrossRef]
21. Singh, R.; Bhatia, H.; Prakash, P.; Debroye, E.; Dey, S.; Dehaen, W. Tandem Nenitzescu Reaction/Nucleophilic Aromatic Substitution to Form Novel Pyrido Fused Indole Frameworks. *European J. Org. Chem.* **2021**, *2021*, 4865–4875. [CrossRef]
22. Van Hoof, M.; Bynens, L.; Daelemans, B.; González, M.C.R.; Van Meervelt, L.; De Feyter, S.; Dehaen, W. Octahydropyrimido[4,5-*g*]Quinazoline-5,10-Diones: Their Multicomponent Synthesis, Self-Assembly on Graphite and Electrochemistry. *Chem. Commun.* **2022**, *58*, 7686–7689. [CrossRef] [PubMed]
23. Horsten, T.; Alegbejo Price, T.O.; Van Meervelt, L.; Emery, F.D.S.; Dehaen, W. 2-Imidazolidinone Benzofurans as Unexpected Outcome of the Lewis Acid Mediated Nenitzescu Reaction. *New J. Chem.* **2022**, *46*, 2028–2032. [CrossRef]
24. Allen, G.R. The Synthesis of 5-Hydroxyindoles by the Nenitzescu Reaction. In *Organic Reactions*; John Wiley & Sons, Inc.: Hoboken, NJ, USA, 2011; Volume 20, pp. 337–454.
25. Granik, V.G.; Lyubchanskaya, V.M.; Mukhanova, T.I. The Nenitzescu Reaction (Review). *Pharm. Chem. J.* **1993**, *27*, 413–438. [CrossRef]

26. Patil, S.; Patil, R.; Miller, D. Synthetic Applications of the Nenitzescu Reaction to Biologically Active 5-Hydroxyindoles. *Curr. Org. Chem.* **2008**, *12*, 691–717. [CrossRef]
27. Allen, G.R.; Pidacks, C.; Weiss, M.J. The Mitomycin Antibiotics. Synthetic Studies. XIV. The Nenitzescu Indole Synthesis. Formation of Isomeric Indoles and Reaction Mechanism. *J. Am. Chem. Soc.* **1966**, *88*, 2536–2544. [CrossRef] [PubMed]
28. Răileanu, D.; Palaghită, M.; Nenitzescu, C.D. Nenitzescu Synthesis of 5-Hydroxyindoles—II. *Tetrahedron* **1971**, *27*, 5031–5047. [CrossRef]
29. Raileanu, D.; Nenitzescu, C.D. Synthesis of 5-hydroxyindoles. I. derivatives of 2-phenyl-k-hydroxyindole. *Rev. Roum. Chim.* **1965**, *10*, 339.
30. Velezheva, V.S.; Kornienko, A.G.; Topilin, S.V.; Turashev, A.D.; Peregudov, A.S.; Brennan, P.J. Lewis Acid Catalyzed Nenitzescu Indole Synthesis. *J. Heterocycl. Chem.* **2006**, *43*, 873–879. [CrossRef]
31. Mukhanova, T.I.; Alekseeva, L.M.; Kuleshova, E.F.; Granik, V.G.; Chemical, C. Synthesis of 3-Acyl-5-Hydroxyindoles and 3-Acyl-5-Hydroxybenzofurans. Influence of Solvent on the Course of the Nenitzescu Reaction. *Pharm. Chem. J.* **1993**, *27*, 136–142. [CrossRef]
32. Lyubchanskaya, V.M.; Savina, S.A.; Alekseeva, L.M.; Shashkov, A.S.; Chernyshev, V.V.; Granik, V.G. The First Example of the Synthesis of 1-Aminoindole Derivatives by the Nenitzescu Reaction. *Russ. Chem. Bull.* **2004**, *53*, 2834–2839. [CrossRef]
33. Kuckländer, U.; Hühnermann, W. Beobachtungen Zum Mechanismus Der Nenitzescu-Reaktion Synthese von 6-Hydroxy-indol-Derivaten. *Arch. Pharm. (Weinheim)* **1979**, *312*, 515–526. [CrossRef]
34. Lyubchanskaya, V.M.; Panisheva, E.K.; Savina, S.A.; Alekseeva, L.M.; Shashkov, A.S.; Granik, V.G. Quinoneimines in the Nenitzescu Reaction. *Russ. Chem. Bull.* **2005**, *54*, 1690–1699. [CrossRef]
35. Kuckländer, U. Beobachtungen Zum Mechanismus Der Nenitzescu-Reaktion. *Tetrahedron* **1972**, *28*, 5251–5259. [CrossRef]
36. Kuckländer, U. Beobachtungen Zum Mechanismus Der Nenitzescu-Reaktion-III Acylwanderungen-I. *Tetrahedron* **1975**, *31*, 1631–1639. [CrossRef]
37. Kuckländer, U. Zum Mechanismus Der Nenitzescu-Reaktion. IV. Synthese Von Benzindol-Derivaten. *Ann. (Justus Liebigs) Chem.* **1978**, *1631*, 129–139. [CrossRef]
38. Schols, D.; Ruchko, E.A.; Lavrenov, S.N.; Kachala, V.V.; Nawrozkij, M.B.; Babushkin, A.S. Structural Analogs of Umifenovir 2. The Synthesis and AntiHIV Activity Study of New Regioisomeric (Trans-2-Phenylcyclopropyl)-1H-Indole Derivatives. *Chem. Heterocycl. Compd.* **2015**, *51*, 978–983. [CrossRef]
39. Kuckländer, U. Beobachtungen Zum Mechanismus Der Nenitzescu-Reaktion-II. *Tetrahedron* **1973**, *29*, 921–927. [CrossRef]
40. Mukhanova, T.I.; Panisheva, E.K.; Lyubchanskaya, V.M.; Alekseeva, L.M.; Sheinker, Y.N.; Granik, V.G. β-(Benzofur-2-Yl)- and (Indol-2-Yl)Enamines in the Nenitzescu Reaction. *Tetrahedron* **1997**, *53*, 177–184. [CrossRef]
41. Shvedov, V.I.; Panisheva, E.K.; Vlasova, T.F.; Grinev, A.N. Synthesis and Aminomethylation of 6-Hydroxyindoles. *Chem. Heterocycl. Compd.* **1973**, *9*, 1225–1227. [CrossRef]
42. Kuckländer, U.; Edoho, J. Zur Entstehung von Pyrrolo [2,3-*f*] Indolen Bei Der Nenitzescu- Reaktion. *Arch. Pharm. (Weinheim).* **1980**, *313*, 582–587. [CrossRef]
43. Horsten, T. Synthesis and Applications of 1,2- and 4,5-Annulated Indoles. Available online: https://lirias.kuleuven.be/handle/123456789/683665 (accessed on 10 December 2021).
44. Parr, R.W.; Reiss, J.A. An Application of the Nenitszescu Reaction to the Synthesis of 1,2-Annulated Indoles and Benz[g]Indoles. *Aust. J. Chem.* **1984**, *37*, 1263–1270. [CrossRef]
45. Hardeland, R.; Pandi-Perumal, S.R.; Cardinali, D.P. Melatonin. *Int. J. Biochem. Cell Biol.* **2006**, *38*, 313–316. [CrossRef] [PubMed]
46. Panisheva, E.K.; Alekseeva, L.M.; Shashkov, A.S.; Granik, V.G. Condensation of P-Benzoquinone with Anilides of β-Aminocrotonic Acid. *Chem. Heterocycl. Compd.* **2003**, *39*, 1013–1017. [CrossRef]
47. Mikerova, N.I.; Panisheva, E.K. Formation of Substituted Benzofuranones-2 by a Nenitzescu Reaction. *Khimiya Geterotsiklicheskikh Soedin.* **1989**, *10*, 1429–1430. [CrossRef]
48. Chun, Y.S.; Ryu, K.Y.; Kim, J.H.; Shin, H.; Lee, S.G. Tandem Blaise-Nenitzescu Reaction: One-Pot Synthesis of 5-Hydroxy-α-(Aminomethylene)Benzofuran-2(3H)-Ones from Nitriles. *Org. Biomol. Chem.* **2011**, *9*, 1317–1319. [CrossRef]
49. Mbala, B.M.; Jacobs, J.; Claes, P.; Mudogo, V.; De Kimpe, N. Investigation towards an Efficient Synthesis of Benzo[*g*]Isoquinoline-1,5, 10(2H)-Triones. *Tetrahedron* **2011**, *67*, 8747–8756. [CrossRef]
50. Armarego, W.L.F.; Chai, C.L.L. *Purification of Laboratory Chemicals, 8th Edition*; Butterworth-Heinemann: Oxford, UK, 2017; Chapter 3; ISBN 9780128054574.
51. Fulmer, G.R.; Miller, A.J.M.; Sherden, N.H.; Gottlieb, H.E.; Nudelman, A.; Stoltz, B.M.; Bercaw, J.E.; Goldberg, K.I. NMR Chemical Shifts of Trace Impurities: Common Laboratory Solvents, Organics, and Gases in Deuterated Solvents Relevant to the Organometallic Chemist. *Organometallics* **2010**, *29*, 2176–2179. [CrossRef]
52. Agilent Technologies UK Ltd. *CrysAlisPro version 1.171.40.25a*; Agilent Technologies UK Ltd.: Yarnton, UK, 2012.
53. Dolomanov, O.V.; Bourhis, L.J.; Gildea, R.J.; Howard, J.A.K.; Puschmann, H. OLEX2: A Complete Structure Solution, Refinement and Analysis Program. *J. Appl. Crystallogr.* **2009**, *42*, 339–341. [CrossRef]
54. Sheldrick, G.M. SHELXT–Integrated speca-group and crystal-structure determination. *Acta Cryst.* **2015**, *A71*, 3–8.
55. Sheldrick, G.M. Crystal structure refinement with SHELXL. *Acta Cryst.* **2015**, *C71*, 3–8.

56. Fan, M.J.; Li, G.Q.; Liang, Y.M. DABCO Catalyzed Reaction of Various Nucleophiles with Activated Alkynes Leading to the Formation of Alkenoic Acid Esters, 1,4-Dioxane, Morpholine, and Piperazinone Derivatives. *Tetrahedron* **2006**, *62*, 6782–6791. [CrossRef]
57. Patrick, J.B.; Saunders, E.K. Studies on the Nenitzescu Synthesis of 5-Hydroxyindoles. *Tetrahedron Lett.* **1979**, *20*, 4009–4012. [CrossRef]